Polarity proteins PAR6 and aPKC regulate cell death through GSK-3β in 3D epithelial morphogenesis

Minji Kim[1], Anirban Datta[1], Paul Brakeman[2], Wei Yu[1] and Keith E. Mostov[1,*]

[1]Departments of Anatomy, and Biochemistry and Biophysics, University of California School of Medicine, San Francisco, CA 94158, USA
[2]Department of Pediatrics, University of California School of Medicine, San Francisco, CA, USA
*Author for correspondence (e-mail: keith.mostov@ucsf.edu)

Accepted 9 May 2007
Journal of Cell Science 120, 2309-2317 Published by The Company of Biologists 2007
doi:10.1242/jcs.007443

Summary

Epithelial cells are polarized, with an apical surface facing a lumen or outer surface and a basolateral surface facing other cells and extracellular matrix (ECM). Hallmarks of epithelial carcinogenesis include loss of polarity, as well as uncontrolled proliferation and resistance to apoptosis. Are these features controlled by a common molecular mechanism? The partitioning-defective 3 (PAR3)-PAR6-atypical PKC (aPKC) complex is a master regulator that controls polarization in many animal cells. Here we show that PAR6 is involved in apoptosis by regulating aPKC and glycogen synthase kinase 3β (GSK-3β) activity. During epithelial morphogenesis in 3D culture of Madin-Darby canine kidney (MDCK) cells, expression of an N-terminally deleted PAR6 (PAR6ΔN) leads to a significant increase in caspase-dependent cell death by downregulating aPKC activity. Accordingly, inhibition of aPKC in wild-type (WT) MDCK cells with either a cell-permeable PKCζ pseudosubstrate or RNAi promotes apoptosis, which suggests that PAR6 regulates apoptosis via an aPKC-mediated pathway. GSK-3β, a substrate of aPKC, is hyper-activated by expressing PAR6ΔN. GSK-3β inhibitors block PAR6ΔN-induced apoptosis while expression of constitutively active GSK-3β (S9A) promotes apoptosis, which is rescued by ectopic expression of aPKC. We conclude that a PAR6–aPKC–GSK-3β mechanism links cell polarity and apoptosis.

Supplementary material available online at
http://jcs.biologists.org/cgi/content/full/120/14/2309/DC1

Key words: Apoptosis, Cyst formation, Epithelial cell, Polarity

Introduction

The PAR (partitioning defective) complex was first identified in *C. elegans* by its requirement for asymmetric cell division (Guo and Kemphues, 1996) and is involved in various cell polarity-related processes, such as asymmetric cell division (Betschinger et al., 2003; Cai et al., 2003), directed cell migration (Etienne-Manneville and Hall, 2003; Plant et al., 2003), axon specification (Shi et al., 2003) and tight junction formation (Lin et al., 2000; Suzuki et al., 2001). PAR6 has a central scaffolding and regulatory function through its interactions with PAR3, atypical protein kinase C (aPKC) and the Cdc42 GTPase. The N-terminus of PAR6 contains an OPC/PC motif within a PB1 domain that heterodimerizes with aPKC (Hirano et al., 2005). A deletion of the PB1 domain of PAR6 prevents its interaction with aPKC, and results in its incomplete localization (Noda et al., 2003). The PAR6 PB1 domain is followed by a CRIB motif, which engages the GTP-bound form of Cdc42 (Joberty et al., 2000; Lin et al., 2000). In addition to binding to PAR3 via a PDZ domain (Joberty et al., 2000), PAR6 interacts with at least two additional proteins, Lgl (Plant et al., 2003; Yamanaka et al., 2003) and PALS (Hurd et al., 2003), components of the Scribble-Dlg and Crumbs-PATJ polarity complexes, respectively.

Atypical PKC isozymes λ (ι in human) and ζ, which are 72% identical (Akimoto et al., 1994), have been implicated in several signaling pathways, including cell polarity, cell survival and cell differentiation. P62/ZIP, another protein that interacts with the N-terminus of aPKC, has been shown to recruit aPKC into a TNF-α receptor complex and an NGF receptor complex, transducing signals for cell survival (Mamidipudi and Wooten, 2002; Sanz et al., 1999). PKCζ has also been described to protect cells against FasL-induced apoptosis in Jurkat cells (Leroy et al., 2005). Recent studies have linked inappropriate expression of aPKCι to the development of human non-small cell lung cancer (Regala et al., 2005). PKCλ$^{-/-}$ mice are known to be embryonic lethal at very early stages (Bandyopadhyay et al., 2004; Soloff et al., 2004). Thus, aPKC has been implied to be closely related to the signaling pathways that regulate cell survival.

Three-dimensional (3D) epithelial culture systems, which allow epithelial cells to organize themselves into structures that resemble their in vivo architecture, have emerged as unique models that allow investigation of the orientation of epithelial cell polarity and other signaling pathways. Although lumen formation can spontaneously occur within small epithelial clusters coinciding with the establishment of apico-basal polarity (Debnath and Brugge, 2005; Hall et al., 1982; O'Brien et al., 2002), apoptosis also contributes to lumen formation in several 3D models. Indeed, apoptotic cells are present in the developing lumen of salivary gland and mammary spheroids, as well as Madin-Darby canine kidney (MDCK) cysts (Debnath et al., 2003; Hoffman et al., 1996; Huang et al., 1999; Lin et al., 1999).

Using this model system, we now demonstrate that the

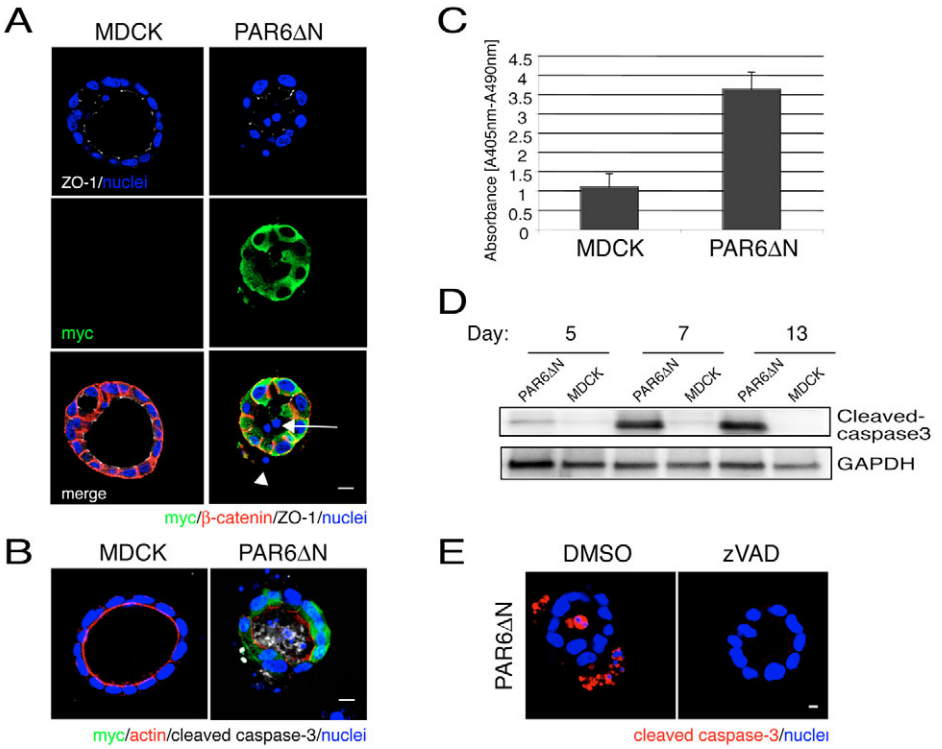

Fig. 1. PAR6ΔN promotes apoptosis in MDCK cystogenesis. (A,B) Wild-type MDCK and Myc-tagged PAR6ΔN-expressing stable cell lines grown on collagen for 7 days were fixed, permeabilized and immunostained for Myc (green), β-catenin (red) and ZO-1 (white) (A) and for Myc (green), actin (red) and cleaved caspase-3 (white) (B). White arrow and arrowhead indicate dead cells in A. Nuclei are shown as blue in all figures. (C) The levels of apoptosis were measured using a cell death ELISA. Results are the mean±s.d. of three experiments. (D) Wild-type MDCK and PAR6ΔN lysates isolated from cysts were prepared at different time points (day 5, 7 and 13) and then analyzed for activation of caspase-3 using cleaved caspase-3 and GAPDH antibodies (loading control). (E) PAR6ΔN cysts were treated with either a carrier (DMSO) or caspase inhibitor, zVAD-fmk (50 μM) three times at day 0, 4 and 6 and immunostained for cleaved caspase-3 (red) at day 7, as described in A. Bars, 10 μm.

PAR6-aPKC complex regulates cell death and/or proliferation during MDCK cyst formation via glycogen synthase kinase 3β (GSK-3β). PAR6ΔN expression suppresses aPKCλ and promotes GSK-3β activity, causing increased apoptosis. Our data suggest that the polarity protein PAR6-aPKC complex plays a surprising and critical role in controlling cell survival.

Results

An N-terminally deleted PAR6 (PAR6ΔN) induces increased apoptosis

Previous work has shown that overexpression of PAR6B or a mutant PAR6B lacking the N-terminus (containing residues 102-373; PAR6ΔN) inhibits TJ (tight junction) assembly during formation of polarity in a calcium switch assay in 2D (monolayer) culture (Gao et al., 2002). Here we used MDCK cells grown as cysts in 3D gels of extracellular matrix, which more closely resembles in vivo conditions. We embedded cells that stably express Myc-tagged PAR6ΔN in collagen gels and allowed cysts to develop for 7 days. While control cysts had a uniform monolayer surrounding a hollow lumen, PAR6ΔN cysts had multilayers of cells in the wall and cells in the cysts. The PAR6ΔN cells forming the outer layer appeared at least somewhat polarized, with ZO-1 localized to the TJ region between apical and basolateral surfaces, and β-catenin at lateral surfaces (Fig. 1A). These data differ somewhat from results previously reported for MDCK cells expressing PAR6ΔN and grown as a 2D monolayer on filters. The reason for this difference is probably due to the well-known differences in MDCK behavior between 2D and 3D culture. Overexpression of wild-type PAR6 or PAR6 containing a mutation in the PDZ domain, which does not bind PAR3, yielded cysts that were not detectably different from WT MDCK (M.K., unpublished).

Interestingly PAR6ΔN cysts showed nuclear condensation and fragmentation in some cells both in the lumen and outside the cyst (Fig. 1A, arrowhead and arrow). Results were consistent among three independent clones and the effect was dependent on the level of PAR6ΔN expression (supplementary material Fig. S1). To determine whether these nuclear changes were due to apoptosis we stained cysts for cleaved caspase-3 as a marker of apoptosis. PAR6ΔN cysts exhibited cleaved caspase-3-positive cells in the lumen and periphery (80.9±2.7% of cysts), while only a few (15±2.6%) control cysts exhibited cleaved caspase-3 positive cells (Fig. 1B). An ELISA for cleaved caspase-3 showed a 3.5-fold increase in cell death (Fig. 1C). Based on their rounded morphology, condensed chromatin, and expression of activated caspases, these displaced cells were undergoing apoptotic death. The caspase-3 activity was significantly increased in PAR6ΔN cysts as early as day 5 of culture on collagen and continued for at least 13 days of cyst formation, as shown by immunoblotting for cleaved caspase-3 (Fig. 1D).

To confirm whether caspase is needed for PAR6ΔN-induced apoptosis, we added the permeable caspase inhibitor, zVAD-fmk to PAR6ΔN cysts. DMSO carrier had no effect, whereas zVAD-fmk abolished increased cell death in PAR6ΔN (Fig. 1E). This inhibitory effect of zVAD-fmk on PAR6ΔN-induced apoptosis was also confirmed by in situ cell death detection assay, based on labeling of DNA strand breaks (supplementary material Fig. S2). Taken together, these data show that PAR6ΔN causes caspase-dependent apoptosis during cyst formation. Since PAR6ΔN cysts maintain a normal size compared with the control, we investigated whether proliferation also increased. We therefore immunostained with Ki-67, a marker for cycling cells and found that PAR6ΔN cysts had increased

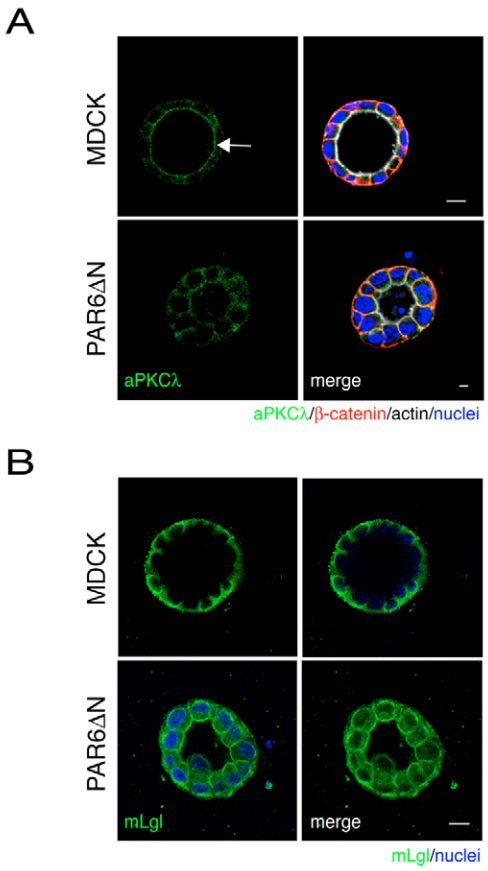

Fig. 2. aPKCλ and mLgl are mislocalized in PAR6ΔN cells. (A) Wild-type MDCK and PAR6ΔN cysts at day 7 were immunolabeled for aPKCλ (green), β-catenin (red) and actin (white). (B) Wild-type MDCK and PAR6ΔN cysts at day 7 were immunolabeled for mLgl (green). Bars, 10 μm.

proliferation, which presumably compensated for increased death (supplementary material Fig. S3). We cannot rule out that the increased proliferation is primary and the increased apoptosis is compensatory.

aPKC activity is required for the regulation of apoptosis during cystogenesis

To better understand the possible mechanism of the effects of PAR6ΔN, we examined the localization of aPKCλ, a protein that forms a polarity-related complex with WT PAR6, but not PAR6ΔN. Although aPKCλ was mostly at the apical plasma membrane in control MDCK cysts (Fig. 2A, upper panel), overexpression of PAR6ΔN delocalized aPKCλ to the cell periphery, which is finely punctate (Fig. 2A, lower panel). Given that a kinase-deficient mutant form of aPKCλ also mostly localizes to the cytosol (Yamanaka et al., 2003), our result suggests that aPKC activity may play a crucial role for aPKCλ localization.

Since our antibody against PAR6 does not work for staining cysts, we observed the localizations of GFP-PAR6 and GFP-PAR6ΔN (supplementary material Fig. S4). GFP-PAR6B partially localized at the apical region, similarly to aPKCλ (supplementary material Fig. S4, upper arrow). However, in cells with a higher expression level, more of the GFP-PAR6B is cytoplasmic (supplementary material Fig. S4, arrowhead). The localization of GFP-PAR6ΔN showed a similar pattern of accumulation at the apical region of cells in cysts (supplementary material Fig. S4, lower arrow).

Lethal giant larvae (Lgl), a protein that interacts with both PAR6 and aPKC and which functions as a substrate of aPKC, is normally found at the basolateral plasma membrane in an aPKC activity-dependent manner (Chalmers et al., 2005; Hutterer et al., 2004; Yamanaka et al., 2003). We observed that overexpression of PAR6ΔN delocalized the mammalian Lgl (mLgl) from the basolateral plasma membrane partially to the cytosol and partially to apical plasma membrane (Fig. 2B, lower panel). This is consistent with the observation that the localization of aPKC is altered by overexpression of PAR6ΔN and indicates that although ZO-1 and β-catenin are correctly polarized, PAR6ΔN induces some degree of alteration in polarity in mature 3D cysts.

These data also raised the possibility that PAR6ΔN expression caused an increase in apoptosis by altering the activity of aPKC. aPKC has been implicated not only in cell polarity but also in cell survival. Earlier work has shown that the N-terminal region of PAR6 is essential for cell transformation by oncogenic Ras or Rac1 (Qiu et al., 2000). To investigate the mechanism by which PAR6ΔN mediates apoptosis, we determined that aPKC is phosphorylated at residues Thr410/403, which provides an indicator of kinase activity (autophosphorylation) of aPKCλ. We found that aPKCλ Thr410/403 phosphorylation was decreased by ~40% in PAR6ΔN cysts (Fig. 3A).

To confirm that increased apoptosis resulted from a reduction in aPKC activity, we used a cell-permeable, myristoylated PKCζ pseudosubstrate peptide (ZI), which directly inhibits aPKC autophosphorylation and transactivation. ZI is commonly used to block both aPKCζ and aPKCλ isoforms because of their high homology. MDCK cells predominantly express aPKCλ. We incubated WT MDCK with 40, 50 or 60 μM ZI (or the non-myristoylated form as a control), starting at day 4 of cyst formation, when epithelial polarity was already established. Apoptotic cells were dose-dependently increased by ZI treatment (Fig. 3B,C). Earlier addition of ZI at the time of plating showed much higher apoptosis, reaching 95% at 60 μM (M.K., unpublished).

As an alternative approach to reduce aPKC function, we transiently transfected MDCK cells with an aPKCλ RNAi construct (Suzuki et al., 2004). The RNAi effect peaks at day 3, reducing its level to less than 10% according to western-blot analysis (Fig. 4A). We therefore grew the cysts in Matrigel, which allows cysts to form much faster than in collagen. In control cysts after 3 days in Matrigel, ZO-1 was localized at the TJ and aPKCλ was enriched at the apical region, which is consistent with our previous results with cysts grown in collagen (Fig. 4B, upper). Cysts transfected with aPKCλ RNAi (but otherwise WT, i.e. not transfected with PAR6ΔN) lost apical staining for aPKCλ and displayed activated caspase-3 in the center of lumen (Fig. 4B, lower). The apoptotic cells were increased in a dose-dependent manner, showing 50% of cysts were affected by 5 μg of aPKCλ RNAi (Fig. 4C). Taken together, these data suggest that PAR6ΔN causes increased apoptosis by inactivation of aPKCλ and that suppression of aPKCλ induces apoptosis

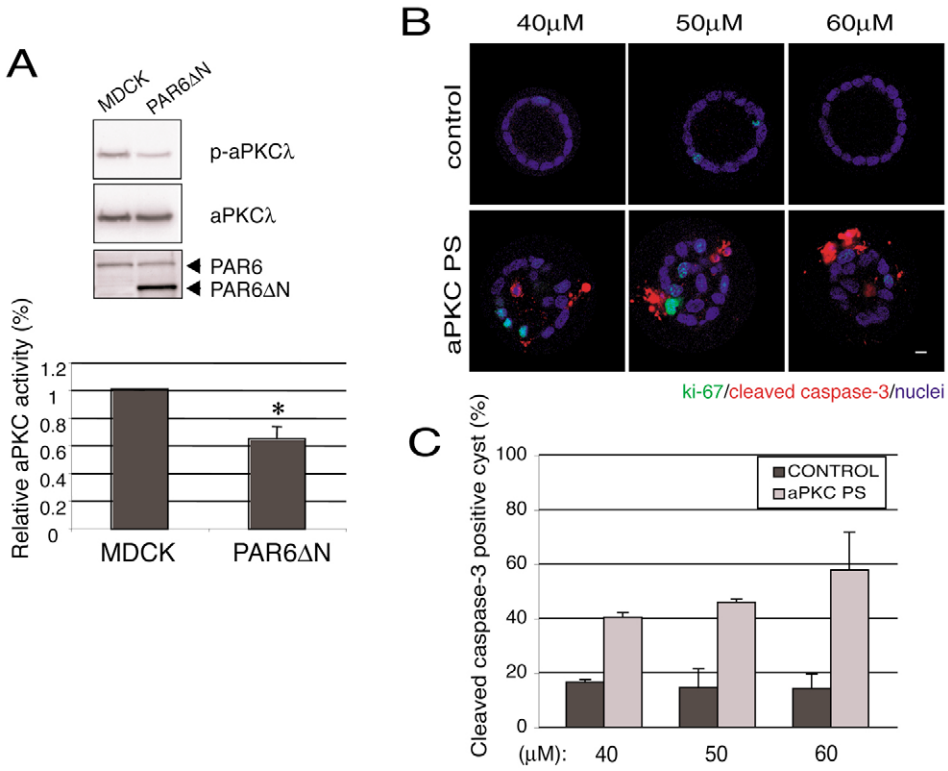

Fig. 3. Reduced aPKCλ activity results in increased cell death in PAR6ΔN cells. (A) aPKCλ activity and PAR6 expression levels were analyzed in wild-type MDCK and PAR6ΔN cells by immunoblot using, respectively, phospho-aPKCλ, total-aPKCλ and PAR6B antibodies. The quantification of three independent experiments is depicted. **P*<0.05. (B) MDCK cysts grown in collagen were treated with either the non-myristoylated (control) or myristoylated form of aPKCζ pseudosubstrate peptide, at the indicated concentrations, at day 4; aPKCζ pseudosubstrate-containing media were refreshed at day 6. Immunostaining with Ki-67 (green) and cleaved caspase-3 (red) were performed at day 7. Bar, 10 μm. (C) Percentage of cysts containing apoptotic cells was quantified by cleaved caspase-3 staining comparing control and aPKC inhibitor-treated cells. Results are the mean±s.d. of three experiments.

during otherwise normal cyst development. These results are consistent with a report that aPKCλ depletion caused increased cell death at the gastrula stage in *Xenopus* development (Chalmers et al., 2005; Moscat and Diaz-Meco, 2000).

Cells in aPKCλ RNAi cysts were at least somewhat polarized, as indicated by the correct localization of ZO-1. This differs from a previous report showing that aPKCλ RNAi in 2D cultures of MDCK inhibited TJ formation (Suzuki et al., 2004). The differences may be due to our use of 3D culture in Matrigel, differing extents of depletion or other factors.

GSK-3β functions downstream of PAR6-aPKC as the mediator of cell death signals

A downstream target of the PAR6-PKCζ-Cdc42 complex in the regulation of migrating astrocyte polarity is GSK-3β (Etienne-Manneville and Hall, 2003). Recent studies have shown that upregulation of GSK-3β activity can lead to cell death and aberrant neuronal migration in primary neuron cultures (Maggirwar et al., 1999; Tong et al., 2001). To test whether GSK-3β is involved in PAR6-aPKC-mediated apoptosis, we examined activation of GSK-3β. Phosphorylation of GSK-3β at serine-9 inhibits its activity. In PAR6ΔN cysts, phosphorylation of GSK-3β is decreased, indicating that GSK-3β is more active (Fig. 5A). LiCl and SB216763, inhibitors of GSK-3, partially, but significantly, reversed the increased apoptosis induced by PAR6ΔN (Fig. 5B). With PAR6ΔN alone, only 25.3% of PAR6ΔN cysts had no activated caspase-3-positive cells, whereas with SB216763 or LiCl, 51.2 or 67.3% of cysts, respectively, had no activated caspase-3 positive cysts ($P<0.05$). This is consistent with the notion that GSK-3β has a proapoptotic function in mammalian cells (Hetman et al., 2000; Pap and Cooper, 1998) and GSK-3β function is required for apoptosis of nurse cells during gametogenesis (Rentzsch et al., 2005).

As an additional way of examining the role of GSK-3β in apoptosis, we infected MDCK cells with recombinant adenovirus expressing WT or mutant GSK-3β and confirmed expression of the constructs by western blotting of the HA epitope tag on the constructs (Fig. 6C). Ad–HA–GSK-3β(K85M) encodes a kinase-dead form of the enzyme, while Ad–HA–GSK-3β(S9A) encodes a mutant that cannot undergo inhibitory phosphorylation at Ser9. In contrast to Ad-LacZ or Ad–HA–GSK-3β(K85M), expression of Ad–HA–GSK-3β(S9A) led to increased apoptosis in MDCK cells that had not been transfected with PAR6ΔN (Fig. 6A,B). These results strongly suggest the involvement of GSK-3β-mediated cell death in cyst formation. In addition, this phenotype is partially rescued by co-expression of wild-type aPKCλ (Fig. 7A,B). It has been reported that treatment with a aPKC inhibitor abrogated GSK-3β phosphorylation (Wu et al., 2006). To further confirm this, we inhibited aPKC activity using ZI and measured GSK-3β activity by staining with phospho-GSK-3β. The amount of phospho-GSK-3β was decreased, as indicated by some cells that had no visible staining (arrow in Fig. 7C). Conversely, overexpression of wild-type aPKCλ increases GSK-3β phosphorylation (Fig. 7D, arrow indicates cells with overexpression of GFP- aPKC and increased phospho-GSK-3β). Taken together, our results strongly suggest that PAR6-aPKC regulates apoptosis through modulation of GSK-3β activity.

To analyze a potential mechanism whereby active GSK-3β exerts its apoptotic effects, we measured phosphorylation of Jun N-terminal kinase (JNK). JNK plays an important role in signal transduction pathways: JNK expression is increased in response to stress, cytokines and many anti-cancer drugs (Chen

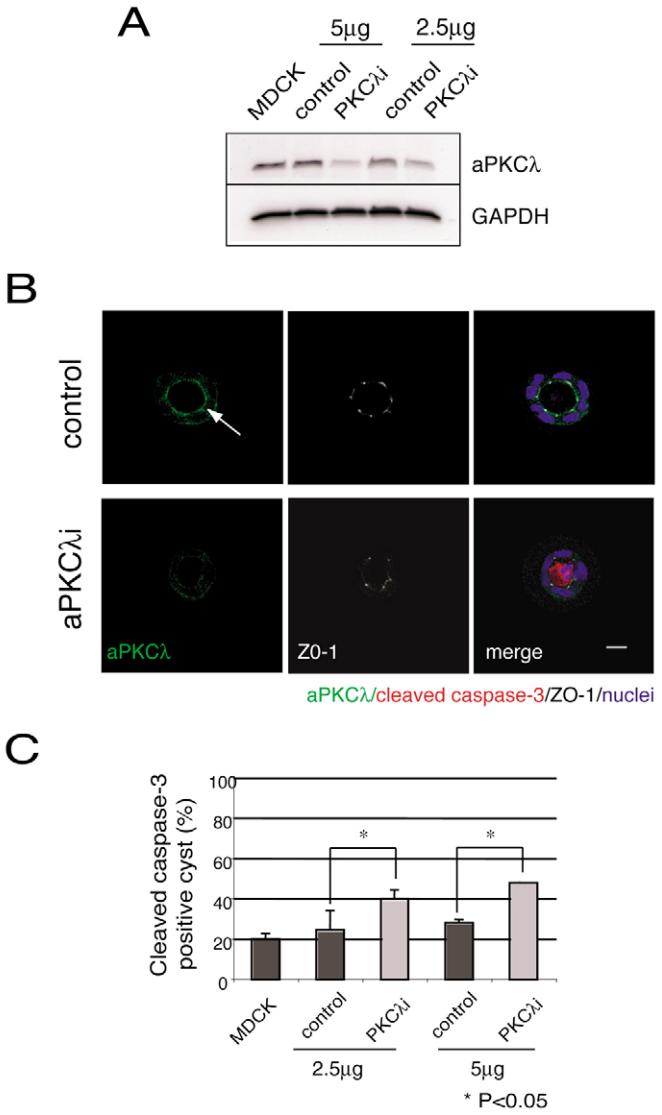

Fig. 4. aPKCλ inhibition by RNAi mimics the effect of PAR6ΔN on apoptosis. (A) MDCK cells transfected with either an empty vector (control) or pSuper-aPKCλ RNAi were grown on Matrigel for 3 days and subjected to immunoblotting with total-aPKCλ (upper panel) and GAPDH (lower panel). (B) Control and aPKCλ RNAi MDCK cells grown on Matrigel were immunostained with aPKCλ (green; left), ZO-1 (white; middle) and cleaved caspase-3 (red; right). Bar, 10 μm. (C) Percentage of apoptotic cells was evaluated by cleaved caspase-3 staining comparing control and aPKCλ RNAi MDCK cells. Results are the mean±s.d. of three experiments.

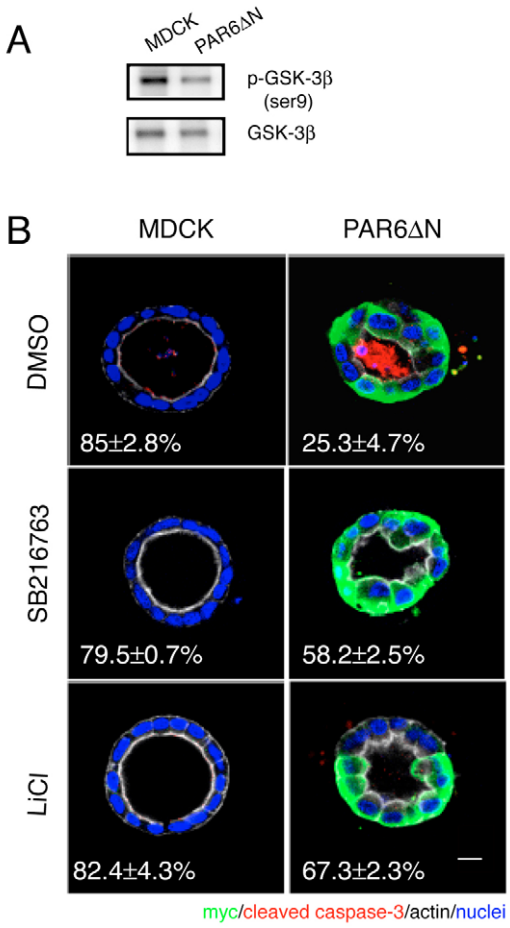

Fig. 5. GSK-3β is hyperactivated in PAR6ΔN cells and GSK-3β inhibitors suppress PAR6ΔN-induced apoptosis. (A) Immunoblot of phospho-GSK-3β (Ser9) (upper panel) and total GSK-3β (lower panel) from wild-type MDCK and PAR6ΔN total SDS-lysates. (B) Wild-type MDCK and PAR6ΔN cells grown in collagen for 4 days were then cultured in the presence of 20 μM SB216763, 50 μM LiCl or vehicle (DMSO) and immunostained with Myc (green), cleaved caspase-3 (red) and actin (white) at day 7. Values shown at the bottom of each panel indicate the percentage of cysts lacking cleaved caspase-3 staining (mean±s.d. of three experiments). Bar, 10 μm.

et al., 1996; Oshima et al., 1996; Stone and Chambers, 2000), and JNK is also required for some forms of stress-induced apoptosis (Tournier et al., 2000). By contrast, the constitutive biological function of JNK is to promote cell survival or growth (Ip and Davis, 1998). In agreement with a previous study showing that JNK is activated after MDCK detachment (Hideshima et al., 2003), we found that JNK was activated in PAR6ΔN (Fig. 7E). We attempted to inhibit JNK pharmacologically, for example with SP-600125, which is the most widely used JNK-specific inhibitor. However, we found that even a concentration of SP-600125 of 20 μM inhibited viability, which prevented us from determining whether there was a specific effect on GSK-3β-regulated apoptosis (M.K., unpublished). It has been suggested that GSK-3β acts as a positive mediator of stress- and proinflammatory cytokine-induced JNK activation (Kim et al., 2003). It is also interesting to note a recent report that JNK signaling is activated in polarity-deficient cells and, in the presence of oncogenic Ras, JNK switches its proapoptotic role to a progrowth effect (Igaki et al., 2006). Taken together, our results are consistent with the idea that PAR6–aPKC–GSK-3β altered JNK activity, which may have compromised cell survival during MDCK cyst formation.

Discussion

Despite recent studies revealing a link between epithelial polarization and proliferation (Aranda et al., 2006; Bilder, 2004), the role of PAR6 as an effector of signal transduction

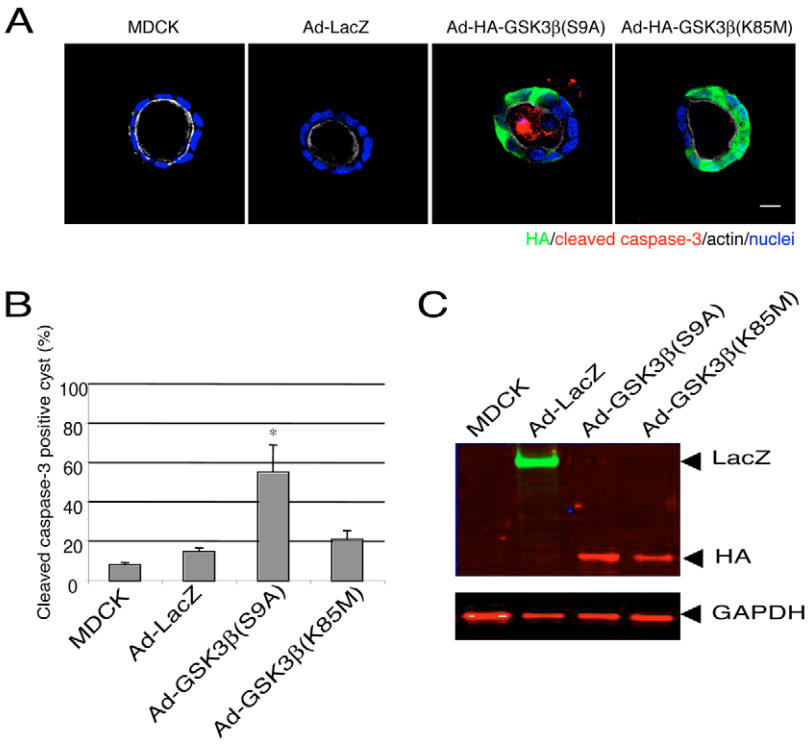

Fig. 6. GSK-3β activity is crucial for apoptosis in MDCK cystogenesis. (A) Wild-type MDCK cells were cultured on Matrigel (72 hours) and infected with Ad-LacZ, Ad–HA–GSK-3β (S9A), Ad–HA–GSK-3β (K85M) for 24 hours, or not infected (MDCK control). Immunostaining analysis was performed with HA (green), cleaved caspase-3 (red) and actin (white). Bar, 10 μm. (B) The percentage of cysts containing apoptotic cells was quantified by cleaved caspase-3 staining. Results are the mean±s.d. of three experiments. **P*<0.05 compared with either Ad-LacZ or Ad–HA–GSK-3β (K85M). (C) MDCK cysts infected with Ad-LacZ, Ad–HA–GSK-3β (S9A), or Ad–HA–GSK-3β (K85M) were subjected to immunoblot with β-gal (green), HA (red) and GAPDH (red).

in this area is only just beginning to be understood (Aranda et al., 2006). In the present study, we found that overexpression of an N-terminal deletion mutant of PAR6 induced significant cell death during MDCK cyst formation; this resulted from the inactivation of aPKC and hyperactivation of GSK-3β.

Lumen formation by apoptosis, which occurs in 3D cultures of kidney (O'Brien et al., 2002) and mammary epithelium (Debnath et al., 2002; Muthuswamy et al., 2001), is believed to reflect physiological death occurring during development and homeostasis of these tissues. Alterations in cell death during development result in compromised functioning of the developing organism and are also involved in a number of pathological processes, such as cystic diseases of the kidney (e.g. polycystic kidney disease) and other organs, as well as cancer. Combined inhibition of apoptosis and hyper-stimulation of proliferation leads to a lumen-filling phenotype in a model of early mammary carcinogenesis (Debnath et al., 2002). Cells in the middle of the lumen may die due to anoikis, a type of cell death caused by detachment from the basement membrane. However, PAR6ΔN produced activated caspase-positive dead cells both in the lumen and outside the cysts, a phenomenon that, to our knowledge, was not reported in work in mammary cyst lumen filling. The apoptotic cells outside the MDCK cysts may result from basal extrusion of dead cells (Gibson and Perrimon, 2005).

Regulation of apoptosis in 3D tissues is tightly coupled to cell-ECM and cell-cell interactions (Zahir and Weaver, 2004). Seminal work indicated that disrupting polarity organization renders epithelial structures more susceptible to apoptosis (Weaver et al., 2002). In this study we took advantage of the 3D MDCK cell system, which have well-developed and extensively characterized polarity. By contrast, many of the mammary cell lines used in 3D culture (e.g. MCF10A) lack TJ, are apparently less well polarized than MDCK, and are therefore probably less suitable for studying the connection between polarity and apoptosis.

PAR6ΔN produced only a partial disruption of polarity in cysts. ZO-1 and β-catenin were normal, although mLgl and aPKCλ were mislocalized. aPKC phosphorylates Lgl and restrict its activity to the basal side so that determinants are only recruited to that portion of the cell cortex in *Drosophila* (Betschinger et al., 2003). Similar observations have been described in MDCK (Musch et al., 2002). This model of regulation of mLgl localization by aPKC is reminiscent of the finding that Par1 localization is also regulated in a phosphorylation-dependent manner by aPKC (Hurov et al., 2004; Suzuki et al., 2004). Despite the localization defects of aPKC and mLgl, however, PAR6ΔN does not induce defects in cyst formation (Fig. 2). This is consistent with a previous study that a non-phosphorylated form of mLgl does not markedly influence the development of a polarized phenotype in MDCK cells, although the localization of the mutant protein is affected (Musch et al., 2002). We cannot completely exclude the possibility that the mislocalization of mLgl induced by PAR6ΔN is somehow responsible for the increase in apoptosis that we observe in response to PAR6ΔN.

The mechanism by which the kinase activity of aPKC is regulated has not been clearly determined. Our finding that PAR6ΔN expression blocks autophosphorylation of aPKC and reduces the activity of aPKC (Fig. 3A) raises the possibility that PAR6ΔN expression induces a conformational change of the PAR6-aPKC complex to make the PB1 domain of aPKC free, which then functions as a dominant negative (Regala et al., 2005). Alternatively, others have proposed a model in which PAR6 exists in an equilibrium between an inactive and an active state, and activation can be artificially induced by removing the N-terminal domain of PAR6 (Gao et al., 2002).

We suggest that PAR6ΔN activates GSK-3β through the

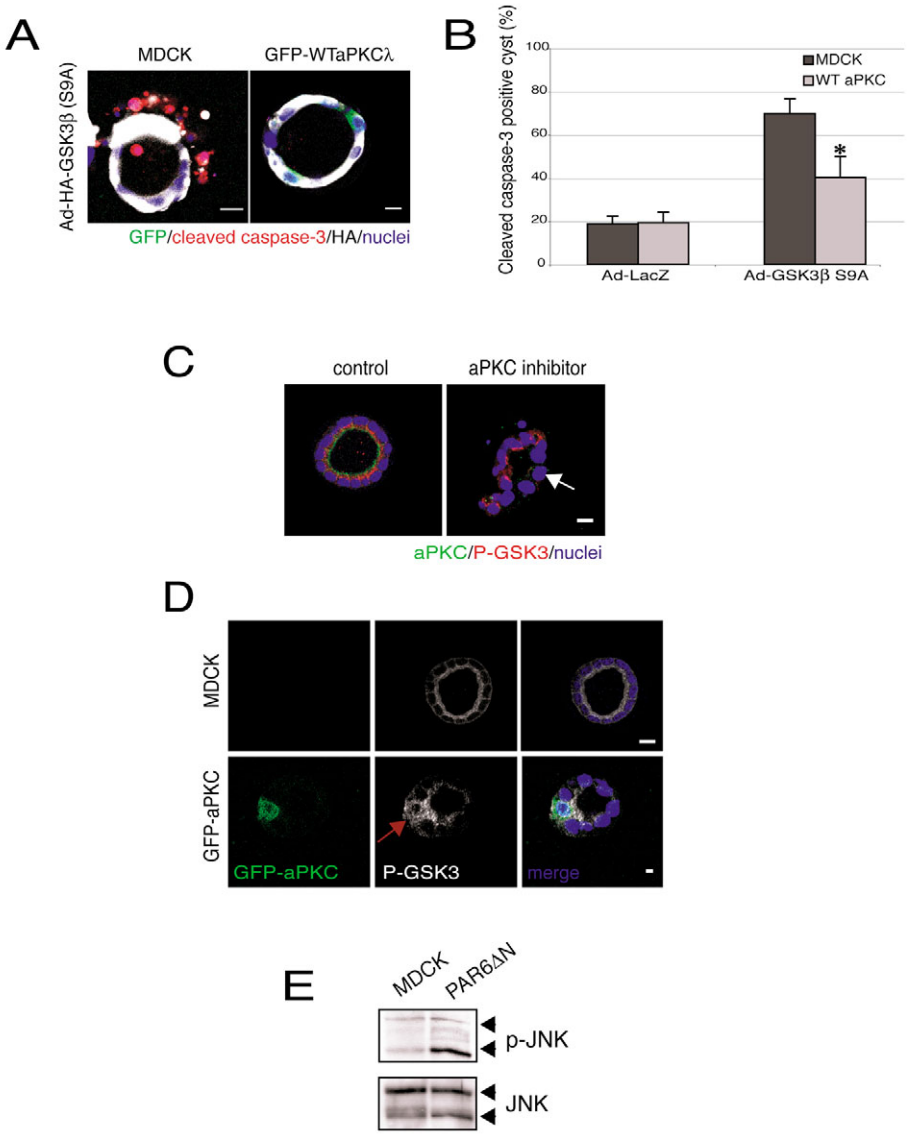

Fig. 7. Cell death induced by active GSK-3β is partially rescued by expression of aPKCλ. (A) Wild-type MDCK and GFP-aPKCλ cells were cultured on Matrigel (72 hours) and infected with Ad–HA–GSK-3β (S9A). Immunostaining analysis was performed with GFP (green), cleaved caspase-3 (red) and HA (white). (B) Wild-type MDCK and GFP-aPKCλ cells were cultured on Matrigel (72 hours) and infected with Ad-βgal or Ad–HA–GSK-3β (S9A). The percentage of cysts containing apoptotic cells was quantified by cleaved caspase-3 staining. Results are the mean±s.d. of three experiments. (C) MDCK cysts grown in collagen were treated with either the non-myristoylated (control) or myristoylated form of aPKCζ pseudosubstrate peptide at 50 μM at day 4; aPKCζ pseudosubstrate-containing media were refreshed everyday. Immunostaining with aPKCλ (green) and phosphorylated GSK-3β (red) was performed at day 7. (D) Wild-type MDCK and GFP-aPKCλ-overexpressing MDCK cells were embedded into collagen and cultured for 7 days. Immunostaining with GFP-aPKCλ (green) and phosphorylated GSK-3β (white) was performed at day 7. Bars, 10 μm. (E) Wild-type MDCK and PAR6ΔN lysates at day 7 were subjected to immunoblot of total- and phospho-JNK antibody.

inhibition of aPKC. PKCζ has been shown to phosphorylate GSK-3β in vitro (Etienne-Manneville and Hall, 2003). Work performed in *Xenopus* suggested that LKB1 promotes the inhibition of GSK-3β via PKCζ (Ossipova et al., 2003). A recent report showed that PKCζ inhibitors completely abrogated GSK-3β phosphorylation (Wu et al., 2006). These results support our observation that GSK-3β has a pro-apoptotic function via aPKC.

What downstream molecules might be involved in this pathway? One candidate could be JNK. Indeed we found that JNK was activated in PAR6ΔN cysts (Fig. 7E). Although we could obtain this correlative evidence, we were unable to inhibit JNK pharmacologically or by RNAi (M.K., unpublished) without compromising cell survival. Further work is needed to demonstrate directly a causal relationship. Another candidate could be NF-κB, which has been shown to connect tissue polarity and apoptosis resistance in mammary epithelial cells (MECs) (Weaver et al., 2002). In addition, aPKC mediates the activation of NF-κB (Sanz et al., 1999) and GSK-3β induces apoptosis mediated by inhibition of the NF-κB pathway in astrocytes (Sanchez et al., 2003). However, the incubation of WT MDCK cysts with a cell-permeable soluble peptide SN50, which specifically inhibits nuclear translocation of NF-κB, failed to induce caspase-dependent apoptosis (M.K., unpublished). This suggests that NF-κB is not involved in PAR6–aPKC–GSK-3β-complex-mediated apoptosis.

Here we provide evidence that a PAR6–aPKC–GSK-3β pathway controls not only polarization, but also caspase-dependent cell death. Overexpression of PAR6ΔN leads to reduction of aPKC activity, which in turn causes hyperactivation of GSK-3β; this sequence results in apoptosis in our 3D epithelial culture system. Our results provide a molecular mechanism connecting polarity and apoptosis during epithelial morphogenesis.

Materials and Methods

Materials

The mouse anti-Myc, anti-HA and anti-β-galatosidase (LacZ) antibodies were obtained from Santa Cruz Biotechnology, Convance and Roche respectively. Mouse anti-ZO-1, anti-Ki67 (Zymed), rabbit anti-β-catenin (Santa Cruz Biotechnology), mouse anti-phopho-JNK, rabbit-anti-cleaved-caspase-3, anti-JNK, anti-phospho-PKCλ/ζ and anti-phospho-GSK-3β (Ser9) (all Cell Signaling Technology)

antibodies were used. Mouse anti-PKCλ and anti-GSK-3β antibodies were purchased from BD Biosciences. Mouse anti-glyceraldehyde 3-phosphate dehydrogenase (GAPDH) antibody was purchased from Biodesign International. Rabbit anti-PAR6B and anti-mLgl antibodies were kindly provided by I. Macara (University of Virginia, Charlottesville, VA) and T. Pawson (Samuel Lunenfeld Research Institute, Toronto, Ontario), respectively. Secondary antibodies conjugated to Alexa Fluor-488, -555 and -647 were used for immunostaining experiments (Molecular Probes). Nuclei were labeled with Hoechst 33342 (Molecular Probes). z-VAD-fmk, SB216763 (Calbiochem), LiCl (Fisher) and PKCζ pseudo-substrate (Biosource) were purchased.

Cell culture

Madin-Darby canine kidney (MDCK) cells were maintained in minimal essential medium (MEM) containing Earle's balanced salt solution (Cellgro) supplemented with 5% FBS and antibiotics in 5% CO_2 and 95% air. PAR6ΔN MDCKII stable cell lines were kindly provided by L. Gao (University of Virginia, Charlottesville, VA) and I. Macara and maintained in growth medium with 100 μg of HygromycinB, as in the previous studies (Gao et al., 2002). Mammalian PAR6 was excised from pK-myc (PAR6B) with *Hin*dIII and *Eco*RI and cloned into pEGFP-C3 with *Xho*I and *Eco*RI sites. GFP-PAR6B, GFP-PAR6ΔN or GFP-aPKCλ was transfected by Lipofectamine2000 (Invitrogen). Cyst cultures were prepared as described previously (O'Brien et al., 2001). To treat cysts with inhibitors, z-VAD-fmk was added to the culture medium three times at day 0, 4 and 6. The treatment of aPKCζ pseudosubstrate, SB216763 or LiCl respectively was performed at day 4 and refreshed at day 6 after plating cysts in collagen gel.

RNAi

Generation of pSUPER constructs expressing shRNA targeting canine aPKC has been described previously (Suzuki et al., 2004). For RNAi in MDCK cells, pSUPER constructs expressing gene-specific shRNA were introduced into MDCK cells by nucleofection (Amaxa). 2×10^6 cells were resuspended in 100 μL of nucleofector solution with 2 μg of DNA and electroporated with program T23. After letting cells rest in MEM overnight, either control or aPKC RNAi cells were plated on a matrigel.

Cell death and proliferation analysis

Cells were embedded and cultured in collagen gel on ultra low cluster plates (Costar) at a density of 1×10^5 cells/ml for 7 days. Cells were then lysed for 30 minutes. The level of DNA fragmentation was quantified using the Cell Death ELISA kit (quantifying histone-associated DNA fragments) (Roche). For the cell proliferation assay, after culturing cells as described above, CyQUANT GR dye/cell lysis buffer (CyQUANT cell prolifertion kit) (Molecular Probes) were added. The fluorescence was measured using a filter for 480 nm excitation and 520 nm emission.

Adenovirus infection

MDCK cysts were infected with recombinant adenovirus vectors at an MOI (multiplicity of infection) of 10. For overexpression of GSK-3β mutants, Ad-LacZ (kind gift of S. Maggirwar, University of Rochester Medical Center, Rochester, NY), Ad–HA–GSK-3β (S9A), or Ad–HA–GSK-3β (K85M) (kind gifts of M. Birnbaum, University of Philadelphia, PA) were used. These vectors encode constitutively active GSK-3β mutant containing a serine-to-alanine substitution at residue 9 (GSK-3β S9A) and an enzymatically inactive GSK-3β mutant containing a lysine-to-methionine substitution at residue 85 (GSK-3β K85M). For adenovirus infection, MDCK or GFP-aPKCλ cells were embedded on matrigel for 3 days before infection. After the trypsin treatment, the cells were incubated for 24 hours with 150 μl of the appropriate virus solution. Virus was removed and the cells were overlaid by collagen. Cells were allowed to grow for 4 days in normal growing medium and it was a further 3 days before they were prepared for further examination.

Western blotting

Cysts were isolated from collagen by collagenase treatment for 20 minutes at 4°C. Lysates of isolated cysts were normalized for protein concentration using a BCA assay (Pierce Chemical). The concentration of SDS in the samples was adjusted to 0.5%, and samples were normalized based on the protein concentration of isolated cysts. Proteins were visualized using ECL reagent (Perkin Elmer Life Science). GAPDH was used as control for lysates of the isolated cysts. For detection of adenoviral expression, lysates were immunoblotted for primary antibody followed by a goat anti-mouse IRDye 800 and a goat anti-rabbit Alexa Fluor 680 secondary; they were then analyzed using an Odyssey Infrared Imager (LI-COR).

Immunostaining and confocal microscopy

The procedure for the immunofluorescence staining of cysts cultured in collagen gel was previously described in detail (O'Brien et al., 2001). All images were visualized using a Zeiss 510 LSM confocal microscope and analyzed using the LSM Image Examiner and Adobe Photoshop software. To quantitate cyst undergoing cell death, cysts were stained for cleaved caspase-3 and nuclei and analyzed with a Zeiss 510 LSM. Cysts negatively stained with cleaved caspase-3 were identified as normal cysts. Per condition, 200 cysts were analyzed.

We are grateful to members of the Mostov lab for helpful discussions and J. Debnath for comments on the manuscript. We thank I. G. Macara, T. Pawson, S. B. Maggirwar, and M. Birnbaum for generously supplying reagents. This work was supported by the Tobacco Related Disease Research Program (TRDRP) postdoctoral fellowship (#13FT-0159) to M.K. and by NIH grants to K.E.M.

References

Akimoto, K., Mizuno, K., Osada, S., Hirai, S., Tanuma, S., Suzuki, K. and Ohno, S. (1994). A new member of the third class in the protein kinase C family, PKC lambda, expressed dominantly in an undifferentiated mouse embryonal carcinoma cell line and also in many tissues and cells. *J. Biol. Chem.* **269**, 12677-12683.

Aranda, V., Haire, T., Nolan, M. E., Calarco, J. P., Rosenberg, A. Z., Fawcett, J. P., Pawson, T. and Muthuswamy, S. K. (2006). Par6-aPKC uncouples ErbB2 induced disruption of polarized epithelial organization from proliferation control. *Nat. Cell Biol.* **8**, 1235-1245.

Bandyopadhyay, G., Standaert, M. L., Sajan, M. P., Kanoh, Y., Miura, A., Braun, U., Kruse, F., Leitges, M. and Farese, R. V. (2004). Protein kinase C-lambda knockout in embryonic stem cells and adipocytes impairs insulin-stimulated glucose transport. *Mol. Endocrinol.* **18**, 373-383.

Betschinger, J., Mechtler, K. and Knoblich, J. A. (2003). The Par complex directs asymmetric cell division by phosphorylating the cytoskeletal protein Lgl. *Nature* **422**, 326-330.

Bilder, D. (2004). Epithelial polarity and proliferation control: links from the Drosophila neoplastic tumor suppressors. *Genes Dev.* **18**, 1909-1925.

Cai, Y., Yu, F., Lin, S., Chia, W. and Yang, X. (2003). Apical complex genes control mitotic spindle geometry and relative size of daughter cells in Drosophila neuroblast and pI asymmetric divisions. *Cell* **112**, 51-62.

Chalmers, A. D., Pambos, M., Mason, J., Lang, S., Wylie, C. and Papalopulu, N. (2005). aPKC, Crumbs3 and Lgl2 control apicobasal polarity in early vertebrate development. *Development* **132**, 977-986.

Chen, Y. R., Wang, X., Templeton, D., Davis, R. J. and Tan, T. H. (1996). The role of c-Jun N-terminal kinase (JNK) in apoptosis induced by ultraviolet C and gamma radiation. Duration of JNK activation may determine cell death and proliferation. *J. Biol. Chem.* **271**, 31929-31936.

Debnath, J. and Brugge, J. S. (2005). Modelling glandular epithelial cancers in three-dimensional cultures. *Nat. Rev. Cancer* **5**, 675-688.

Debnath, J., Mills, K. R., Collins, N. L., Reginato, M. J., Muthuswamy, S. K. and Brugge, J. S. (2002). The role of apoptosis in creating and maintaining luminal space within normal and oncogene-expressing mammary acini. *Cell* **111**, 29-40.

Debnath, J., Muthuswamy, S. K. and Brugge, J. S. (2003). Morphogenesis and oncogenesis of MCF-10A mammary epithelial acini grown in three-dimensional basement membrane cultures. *Methods* **30**, 256-268.

Etienne-Manneville, S. and Hall, A. (2003). Cdc42 regulates GSK-3beta and adenomatous polyposis coli to control cell polarity. *Nature* **421**, 753-756.

Gao, L., Joberty, G. and Macara, I. G. (2002). Assembly of epithelial tight junctions is negatively regulated by Par6. *Curr. Biol.* **12**, 221-225.

Gibson, M. C. and Perrimon, N. (2005). Extrusion and death of DPP/BMP-compromised epithelial cells in the developing Drosophila wing. *Science* **307**, 1785-1789.

Guo, S. and Kemphues, K. J. (1996). Molecular genetics of asymmetric cleavage in the early Caenorhabditis elegans embryo. *Curr. Opin. Genet. Dev.* **6**, 408-415.

Hall, H. G., Farson, D. A. and Bissell, M. J. (1982). Lumen formation by epithelial cell lines in response to collagen overlay: a morphogenetic model in culture. *Proc. Natl. Acad. Sci. USA* **79**, 4672-4676.

Hetman, M., Cavanaugh, J. E., Kimelman, D. and Xia, Z. (2000). Role of glycogen synthase kinase-3beta in neuronal apoptosis induced by trophic withdrawal. *J. Neurosci.* **20**, 2567-2574.

Hideshima, T., Hayashi, T., Chauhan, D., Akiyama, M., Richardson, P. and Anderson, K. (2003). Biologic sequelae of c-Jun NH(2)-terminal kinase (JNK) activation in multiple myeloma cell lines. *Oncogene* **22**, 8797-8801.

Hirano, Y., Yoshinaga, S., Takeya, R., Suzuki, N. N., Horiuchi, M., Kohjima, M., Sumimoto, H. and Inagaki, F. (2005). Structure of a cell polarity regulator, a complex between atypical PKC and Par6 PB1 domains. *J. Biol. Chem.* **280**, 9653-9661.

Hoffman, M. P., Kibbey, M. C., Letterio, J. J. and Kleinman, H. K. (1996). Role of laminin-1 and TGF-beta 3 in acinar differentiation of a human submandibular gland cell line (HSG). *J. Cell Sci.* **109**, 2013-2021.

Huang, J., Hardy, J. D., Sun, Y. and Shively, J. E. (1999). Essential role of biliary glycoprotein (CD66a) in morphogenesis of the human mammary epithelial cell line MCF10F. *J. Cell Sci.* **112**, 4193-4205.

Hurd, T. W., Gao, L., Roh, M. H., Macara, I. G. and Margolis, B. (2003). Direct interaction of two polarity complexes implicated in epithelial tight junction assembly. *Nat. Cell Biol.* **5**, 137-142.

Hurov, J. B., Watkins, J. L. and Piwnica-Worms, H. (2004). Atypical PKC phosphorylates PAR-1 kinases to regulate localization and activity. *Curr. Biol.* **14**, 736-741.

Hutterer, A., Betschinger, J., Petronczki, M. and Knoblich, J. A. (2004). Sequential

roles of Cdc42, Par-6, aPKC, and Lgl in the establishment of epithelial polarity during Drosophila embryogenesis. *Dev. Cell* **6**, 845-854.

Igaki, T., Pagliarini, R. A. and Xu, T. (2006). Loss of cell polarity drives tumor growth and invasion through JNK activation in Drosophila. *Curr. Biol.* **16**, 1139-1146.

Ip, Y. T. and Davis, R. J. (1998). Signal transduction by the c-Jun N-terminal kinase (JNK) – from inflammation to development. *Curr. Opin. Cell Biol.* **10**, 205-219.

Joberty, G., Petersen, C., Gao, L. and Macara, I. G. (2000). The cell-polarity protein Par6 links Par3 and atypical protein kinase C to Cdc42. *Nat. Cell Biol.* **2**, 531-539.

Kim, J. W., Lee, J. E., Kim, M. J., Cho, E. G., Cho, S. G. and Choi, E. J. (2003). Glycogen synthase kinase 3 beta is a natural activator of mitogen-activated protein kinase/extracellular signal-regulated kinase kinase kinase 1 (MEKK1). *J. Biol. Chem.* **278**, 13995-14001.

Leroy, I., de Thonel, A., Laurent, G. and Quillet-Mary, A. (2005). Protein kinase C zeta associates with death inducing signaling complex and regulates Fas ligand-induced apoptosis. *Cell. Signal.* **17**, 1149-1157.

Lin, D., Edwards, A. S., Fawcett, J. P., Mbamalu, G., Scott, J. D. and Pawson, T. (2000). A mammalian PAR-3-PAR-6 complex implicated in Cdc42/Rac1 and aPKC signalling and cell polarity. *Nat. Cell Biol.* **2**, 540-547.

Lin, H. H., Yang, T. P., Jiang, S. T., Yang, H. Y. and Tang, M. J. (1999). Bcl-2 overexpression prevents apoptosis-induced Madin-Darby canine kidney simple epithelial cyst formation. *Kidney Int.* **55**, 168-178.

Maggirwar, S. B., Tong, N., Ramirez, S., Gelbard, H. A. and Dewhurst, S. (1999). HIV-1 Tat-mediated activation of glycogen synthase kinase-3beta contributes to Tat-mediated neurotoxicity. *J. Neurochem.* **73**, 578-586.

Mamidipudi, V. and Wooten, M. W. (2002). Dual role for p75(NTR) signaling in survival and cell death: can intracellular mediators provide an explanation? *J. Neurosci. Res.* **68**, 373-384.

Moscat, J. and Diaz-Meco, M. T. (2000). The atypical protein kinase Cs. Functional specificity mediated by specific protein adapters. *EMBO Rep.* **1**, 399-403.

Musch, A., Cohen, D., Yeaman, C., Nelson, W. J., Rodriguez-Boulan, E. and Brennwald, P. J. (2002). Mammalian homolog of Drosophila tumor suppressor lethal (2) giant larvae interacts with basolateral exocytic machinery in Madin-Darby canine kidney cells. *Mol. Biol. Cell* **13**, 158-168.

Muthuswamy, S. K., Li, D., Lelievre, S., Bissell, M. J. and Brugge, J. S. (2001). ErbB2, but not ErbB1, reinitiates proliferation and induces luminal repopulation in epithelial acini. *Nat. Cell Biol.* **3**, 785-792.

Noda, Y., Kohjima, M., Izaki, T., Ota, K., Yoshinaga, S., Inagaki, F., Ito, T. and Sumimoto, H. (2003). Molecular recognition in dimerization between PB1 domains. *J. Biol. Chem.* **278**, 43516-43524.

O'Brien, L. E., Jou, T. S., Pollack, A. L., Zhang, Q., Hansen, S. H., Yurchenco, P. and Mostov, K. E. (2001). Rac1 orientates epithelial apical polarity through effects on basolateral laminin assembly. *Nat. Cell Biol.* **3**, 831-838.

O'Brien, L. E., Zegers, M. M. and Mostov, K. E. (2002). Opinion: Building epithelial architecture: insights from three-dimensional culture models. *Nat. Rev. Mol. Cell Biol.* **3**, 531-537.

Oshima, M., Dinchuk, J. E., Kargman, S. L., Oshima, H., Hancock, B., Kwong, E., Trzaskos, J. M., Evans, J. F. and Taketo, M. M. (1996). Suppression of intestinal polyposis in Apc delta716 knockout mice by inhibition of cyclooxygenase 2 (COX-2). *Cell* **87**, 803-809.

Ossipova, O., Bardeesy, N., DePinho, R. A. and Green, J. B. (2003). LKB1 (XEEK1) regulates Wnt signalling in vertebrate development. *Nat. Cell Biol.* **5**, 889-894.

Pap, M. and Cooper, G. M. (1998). Role of glycogen synthase kinase-3 in the phosphatidylinositol 3-Kinase/Akt cell survival pathway. *J. Biol. Chem.* **273**, 19929-19932.

Plant, P. J., Fawcett, J. P., Lin, D. C., Holdorf, A. D., Binns, K., Kulkarni, S. and Pawson, T. (2003). A polarity complex of mPar-6 and atypical PKC binds, phosphorylates and regulates mammalian Lgl. *Nat. Cell Biol.* **5**, 301-308.

Qiu, R. G., Abo, A. and Martin, G. S. (2000). A human homolog of the C. elegans polarity determinant Par-6 links Rac and Cdc42 to PKCzeta signaling and cell transformation. *Curr. Biol.* **10**, 697-707.

Regala, R. P., Weems, C., Jamieson, L., Khoor, A., Edell, E. S., Lohse, C. M. and Fields, A. P. (2005). Atypical protein kinase C iota is an oncogene in human non-small cell lung cancer. *Cancer Res.* **65**, 8905-8911.

Rentzsch, F., Hobmayer, B. and Holstein, T. W. (2005). Glycogen synthase kinase 3 has a proapoptotic function in Hydra gametogenesis. *Dev. Biol.* **278**, 1-12.

Sanchez, J. F., Sniderhan, L. F., Williamson, A. L., Fan, S., Chakraborty-Sett, S. and Maggirwar, S. B. (2003). Glycogen synthase kinase 3beta-mediated apoptosis of primary cortical astrocytes involves inhibition of nuclear factor kappaB signaling. *Mol. Cell. Biol.* **23**, 4649-4662.

Sanz, L., Sanchez, P., Lallena, M. J., Diaz-Meco, M. T. and Moscat, J. (1999). The interaction of p62 with RIP links the atypical PKCs to NF-kappaB activation. *EMBO J.* **18**, 3044-3053.

Shi, S. H., Jan, L. Y. and Jan, Y. N. (2003). Hippocampal neuronal polarity specified by spatially localized mPar3/mPar6 and PI 3-kinase activity. *Cell* **112**, 63-75.

Soloff, R. S., Katayama, C., Lin, M. Y., Feramisco, J. R. and Hedrick, S. M. (2004). Targeted deletion of protein kinase C lambda reveals a distribution of functions between the two atypical protein kinase C isoforms. *J. Immunol.* **173**, 3250-3260.

Stone, A. A. and Chambers, T. C. (2000). Microtubule inhibitors elicit differential effects on MAP kinase (JNK, ERK, and p38) signaling pathways in human KB-3 carcinoma cells. *Exp. Cell Res.* **254**, 110-119.

Suzuki, A., Yamanaka, T., Hirose, T., Manabe, N., Mizuno, K., Shimizu, M., Akimoto, K., Izumi, Y., Ohnishi, T. and Ohno, S. (2001). Atypical protein kinase C is involved in the evolutionarily conserved par protein complex and plays a critical role in establishing epithelia-specific junctional structures. *J. Cell Biol.* **152**, 1183-1196.

Suzuki, A., Hirata, M., Kamimura, K., Maniwa, R., Yamanaka, T., Mizuno, K., Kishikawa, M., Hirose, H., Amano, Y., Izumi, N. et al. (2004). aPKC acts upstream of PAR-1b in both the establishment and maintenance of mammalian epithelial polarity. *Curr. Biol.* **14**, 1425-1435.

Tong, N., Sanchez, J. F., Maggirwar, S. B., Ramirez, S. H., Guo, H., Dewhurst, S. and Gelbard, H. A. (2001). Activation of glycogen synthase kinase 3 beta (GSK-3beta) by platelet activating factor mediates migration and cell death in cerebellar granule neurons. *Eur. J. Neurosci.* **13**, 1913-1922.

Tournier, C., Hess, P., Yang, D. D., Xu, J., Turner, T. K., Nimnual, A., Bar-Sagi, D., Jones, S. N., Flavell, R. A. and Davis, R. J. (2000). Requirement of JNK for stress-induced activation of the cytochrome c-mediated death pathway. *Science* **288**, 870-874.

Weaver, V. M., Lelievre, S., Lakins, J. N., Chrenek, M. A., Jones, J. C., Giancotti, F., Werb, Z. and Bissell, M. J. (2002). beta4 integrin-dependent formation of polarized three-dimensional architecture confers resistance to apoptosis in normal and malignant mammary epithelium. *Cancer Cell* **2**, 205-216.

Wu, X., Quondamatteo, F., Lefever, T., Czuchra, A., Meyer, H., Chrostek, A., Paus, R., Langbein, L. and Brakebusch, C. (2006). Cdc42 controls progenitor cell differentiation and beta-catenin turnover in skin. *Genes Dev.* **20**, 571-585.

Yamanaka, T., Horikoshi, Y., Sugiyama, Y., Ishiyama, C., Suzuki, A., Hirose, T., Iwamatsu, A., Shinohara, A. and Ohno, S. (2003). Mammalian Lgl forms a protein complex with PAR-6 and aPKC independently of PAR-3 to regulate epithelial cell polarity. *Curr. Biol.* **13**, 734-743.

Zahir, N. and Weaver, V. M. (2004). Death in the third dimension: apoptosis regulation and tissue architecture. *Curr. Opin. Genet. Dev.* **14**, 71-80.

Journal of Cell Science